

Riding velocity and payload conditions affecting weave modal shape: subjective assessment on riding safety

Stefano Armanini, Elisabetta Leo, Marco Ezio Pezzola, Niccolò Taroni

Soluzioni Ingegneria srl, startup of technology innovation

Via Balicco 113, 23900 Lecco, Italy

e-mail: marco.pezzola@si-ita.it

Federico Cheli

Department of Mechanical Engineering, Politecnico di Milano

Via la Masa 1, 20156 Milan, Italy

e-mail: federico.cheli@polimi.it

Abstract

The target of the research is to improve rider safety related to dynamic stability.

By the installation of accelerometers, the identification of the weave vibration mode has been carried out for different vehicles, payloads and riding speeds. The question piloting the research is: can different vehicles, having the same weave modal damping, but characterized by a different vibration shape, being differently rated by users? The answer is affirmative.

It follows how the performed analysis did not limit to the modal damping as stability indicator only, but also investigated the correlation between the shape of vibration and the rider safety assessment.

Key words: vehicle dynamic, motorcycle, driving stability/weave mode, modal damping, vibration mode shape.

Introduction

The target of the research is to improve rider safety related to dynamic instability often cause of accidents involving powered two-wheeled vehicles, as explained in the “UNECE Transport Review of Road Safety” [1]. Particular gravity is due to rapid increasing presence of riding critical situations that may occur due to the always higher complexity of urban riding scenarios.

As explained by Prof. Cossalter at Al. [2], the motorcycle is a complex strongly non-linear mechanical system that presents many difficulties in assessing the behaviour while in motion. An initial study of the vibration modes of a motorcycle led to the isolation of the weave mode and the wobble mode as the most likely to occur during normal use.

Present work approaches the motorcycle stability problem related to the mode named weave by two main steps, aimed both to better comprehend the phenomena and to increase vehicle stability.

The first stage relates to vehicle design phase, the so-called early stage. By the use of a reliable numerical model it is possible to perform targeted sensitivity analysis to limit the testing phase to the promising solutions that may be implemented without getting lost in a multitude of coupling variants to be later verified through a time consuming (and often ineffective) mode. A fully nonlinear, 20 degrees of freedom (DOFs) vehicle model has been implemented, including tires, suspensions, structures’ compliances and payload, such as rider, pillion, side-cases and top case.

The second stage is a new research. It focuses on the experimental evidences acquired by on-field tests. By the installation of multiple accelerometers on different parts of the bike, the experimental identification of the weave vibration mode has been carried out for different vehicles, payload conditions and riding speeds. The question piloting the research was: “... can two different vehicles, having the same weave modal damping, but characterized by a different vibration mode shape, being differently rated by users?...”. The answer is affirmative.

It follows how the performed modal analysis does not limit to the modal damping as stability indicator only, but investigates the correlation between the shape of vibration and the rider assessment on vehicle perceived safety. Some relevant results are shown, highlighting the distinguishing between the weave shape the rider judges to be safer (better) against the one judged less safe (worse), respectively Figure 1 (b) and (c).

Through a bird-eye view of the schematized bike (as a simplified T-shaped, figure 1(a), with y_g = lateral COG displacement, positive on right, shown in black; δ = relative steering angle, positive clockwise, shown in red; σ = yaw, positive clockwise, shown in blue), a different vehicle response is recognizable. In particular, the relative phase of the yaw with respect to the lateral displacement influences the vehicle behavior, giving the rider a different safety perception.

The centrod shape, defined as all the positions assumed by the instantaneous centres of rotation (ICR) of the main body during a whole weave period (red dots), is computed and its shape is discussed against the centre of gravity (CoG) position.

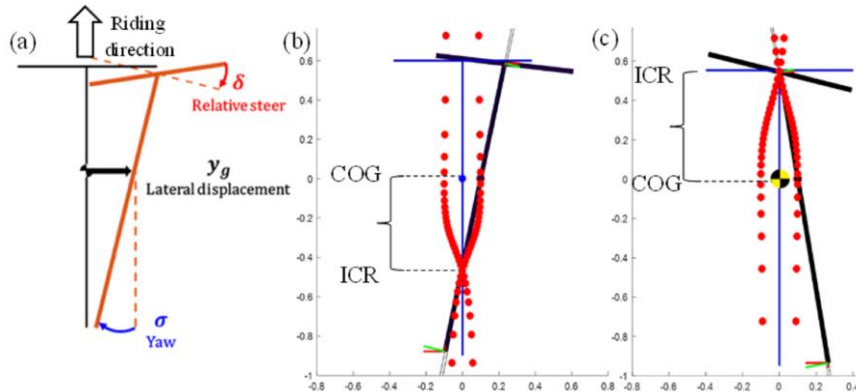


Figure 1 (a): T-bike scheme from bird-eye view; riding direction and degrees of freedom; (b): example of weave with yaw is in-phase with lateral displacement: the ICR meets below the CoG; (c): example of weave with yaw out-of-phase with respect to lateral displacement: the instantaneous centre of rotation (ICR) meets ahead of the centre of gravity (CoG).

The aim is to correlate the centrodome shape with respect to riders' assessment and therefore exploit it as an additional stability indicator. Further investigations will be shown over different payloads conditions (rider only; rider and side bags; rider and pillion) and increasing riding velocity, discovering how, as the payload increases, the yaw becomes more and more in phase with respect to the lateral displacement. It results how the ICR meets below the CoG, being better rated by riders. The higher the riding velocity, instead, the more the yaw relative phase changes from in to counter-phase with respect to lateral displacement. It follows how the ICR meets ahead the CoG, being this time worse rated by riders (vehicle perceived as less safe). The presented innovative approach to motorcycle stability allows to better support new vehicles design, including the rider perception of safety.

1. Experimental set up

During experimental tests three crossover motorcycles from different manufacturers were employed. To quantify payload effects, each of them has been tested in three different conditions: rider solo, with lateral side cases and with passenger plus lateral side cases. The rider was asked to shake his limbs at increasingly steady state step speeds. Since the mechanical system is in a force field arising from the tire contact forces exchanged with the ground, increasing the speed it is possible to vary the system eigenvalues and look at the evolution of the weave mode shape. Each motorcycle was instrumented in the same way. To identify modal damping and weave eigen-vector the following sensors were mounted (Figure 2):

- triaxle MEMS capacitive accelerometers (front (a), handlebar (c), tail (d)) (FS \pm 10 [g], bandwidth 0-2 kHz (5%));
- steering gyroscope (b) (FS \pm 200 [$^{\circ}$ /s], bandwidth 0-100 Hz (5%));
- data logger, up to 6,4 kHz sampling rate, 16-bit analogue channels resolution (d);
- GPS (Global Positioning System) (d).

The sampling frequency of each sensor was set to 200 Hz with Butterworth anti-aliasing filters to cut off high frequency's contributions.

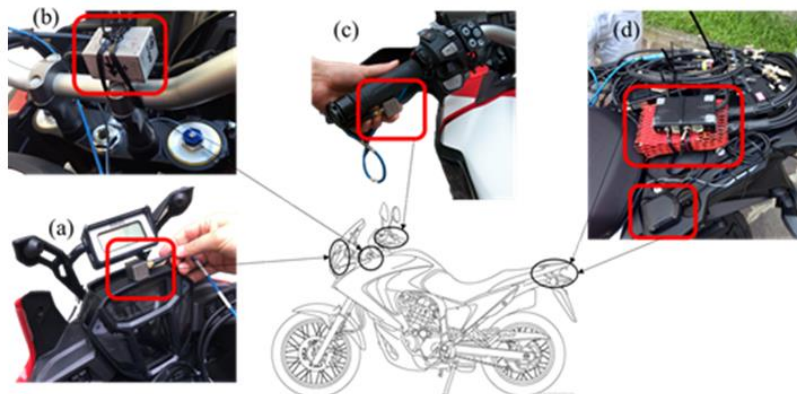


Figure 2 Vehicle set up instrumentation.

2. Experimental methodologies: identification techniques

The experimental approach requires, besides the execution of the tests as described in previous paragraph, also the definition of a methodology for data analysis.

2.1. Eigenvalue: frequency and damping identification

First aim of the latest is the weave frequency and modal damping identification. To do this, we filtered the steering gyroscope signal in the typical weave range (1- 4 Hz). The eigenvalue of the phenomenon was computed by means of Hilbert transform approach ([3], [4]). All the experimental data were processed in order to get damping value and frequency of the oscillation for each step speed. From a statistical point of view, several hip excitation impulses for every speed were considered. The rider was asked to repeat the impulse maneuver at least 3 times for each step speed (Figure 3 (a)).

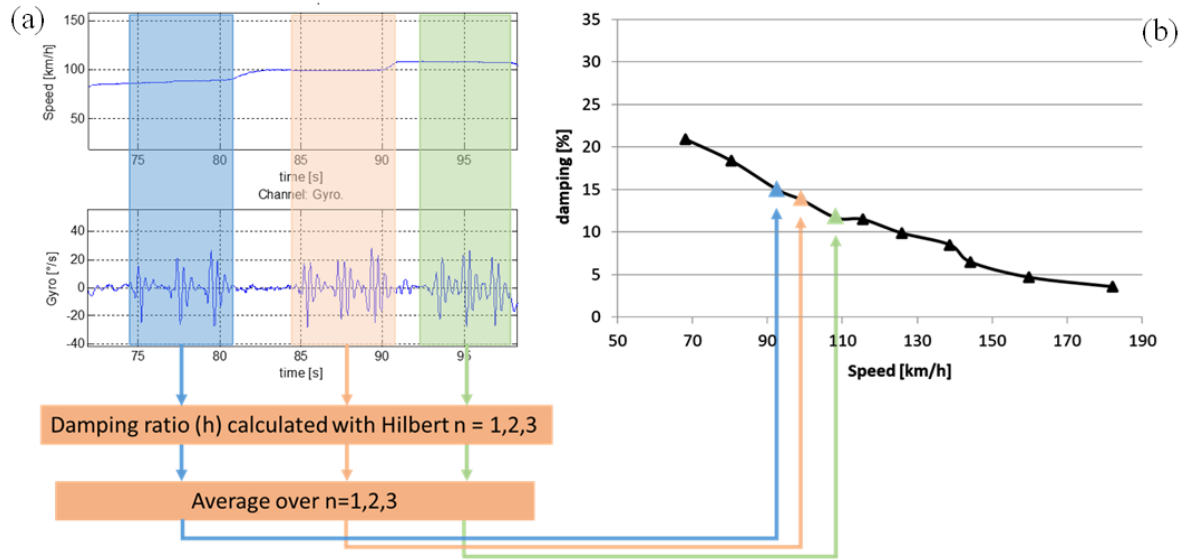


Figure 3 (a) testing procedure aimed to modal damping identification. (b): modal damping versus speed.

Then, the average of the results is computed and collected as the damping ratio over speed graph (Figure 3 (b)). In the following figure 4, two different examples of dynamic response are shown. Those signals refer to the same vehicle, ridden at different speed (left column @ about 130 km/h; right column @ about 190 km/h). The damping ration is computed for both.

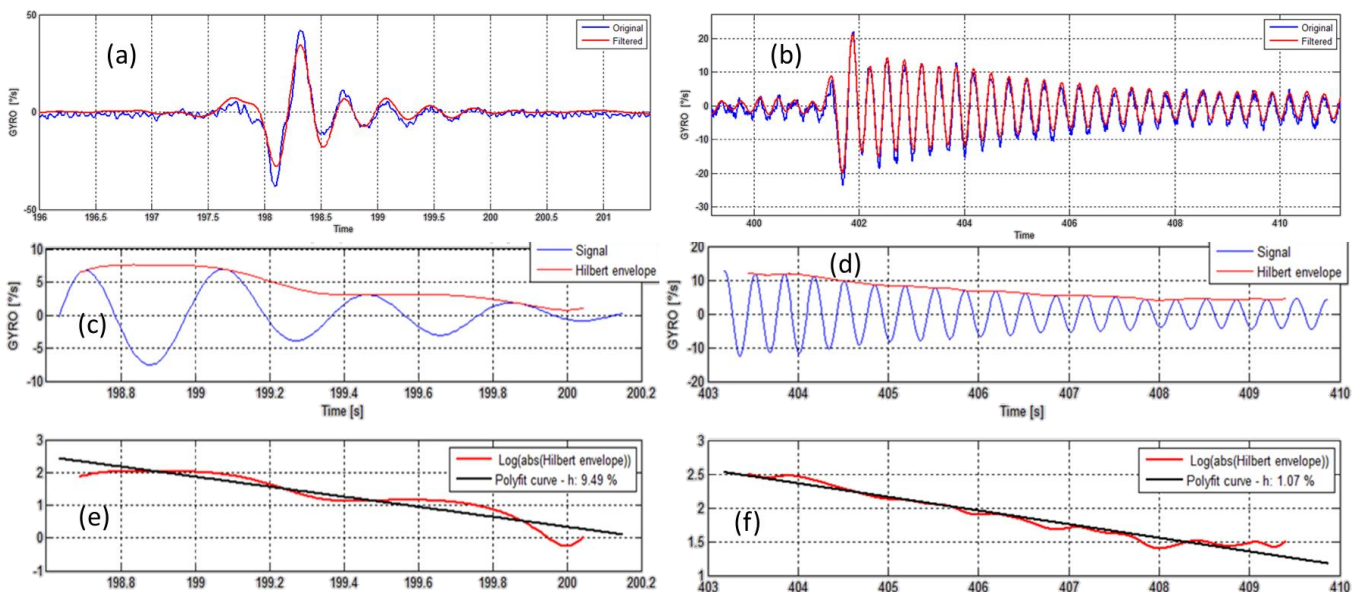


Figure 4 examples of time histories due to impulse response: left column with high damping; right column with low damping. Per row top down: time histories, Hilbert envelope, Hilbert fitting to achieve modal damping.

When the riding speed is low, the weave is characterized by high damping; so far, the oscillations number is poor and the vehicle response suddenly goes back to the original position (a). By applying the Hilbert envelope (c), the damping ration is identifiable (e). In this case, the damping ratio is about 9,5%. On the other hand, riding the vehicle at higher speed, the modal damping decreases; the vehicle, after receiving the impulse excitation, takes many more cycles before going back to the original position (b). Exploiting the same approach, the resulting damping ratio is about 1,1% only. In this condition the vehicle is judge as unsafe due to the very low damping.

2.2. Eigenvector: mode shape reconstruction

In literature [2], the weave is characterized by three mostly involved degrees of freedom (DOFs): the mainframe yaw, the steer relative rotation and the mainframe lateral displacement. The three triaxle accelerometers were mounted on the motorcycles in three significant positions: at the upper front extremity of the main frame (A), at the extremity of the handlebar (B) and on the tail of the main frame (O) (Figure 5). Data rotation from mounting position reference system to motorcycle one has been applied through the Cardanic transformation matrix. To obtain the DOFs, the signals coming from the accelerometers were integrated twice, achieving the displacement of the points A, B and O in three perpendicular di-reactions. For the sake of simplicity, a scheme of the motorcycle has been created, called T-bike (Figure 5): it schematizes the top eye view.

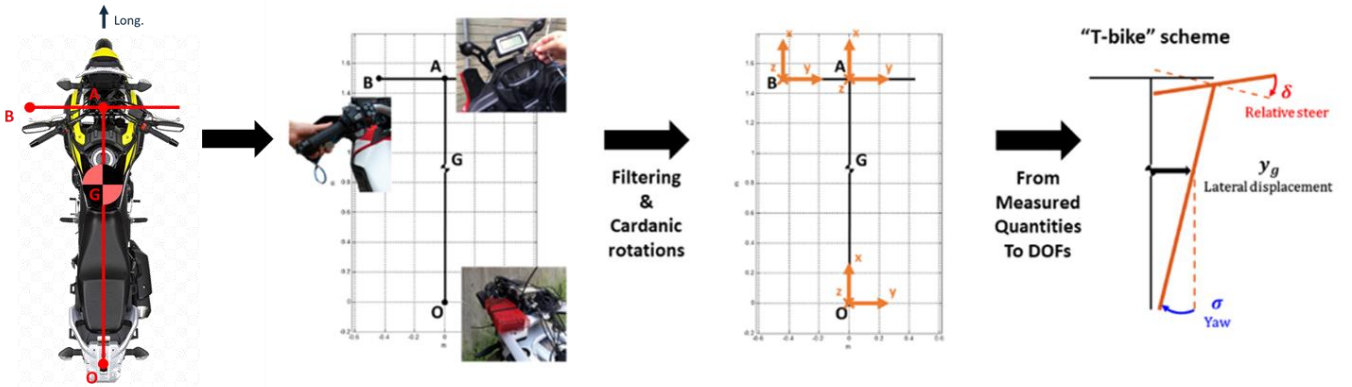


Figure 5 (left to right) from signals acquired by the three installed accelerometers mounted respectively on: A = steering head, B=handlebar extremity and O=tail, to degrees of freedom identification: σ = yaw, y_g = lateral displacement and δ = relative steer.

The degrees of freedom are computed with the following conventions, according to motorcycle reference system:

- σ = yaw positive clockwise, represented in blue;
- δ = relative steer positive clockwise, represented in red;
- y_g = lateral displacement positive rightwards, represented in black.

In the following Figure 6, an example of the DOFs identification is shown.

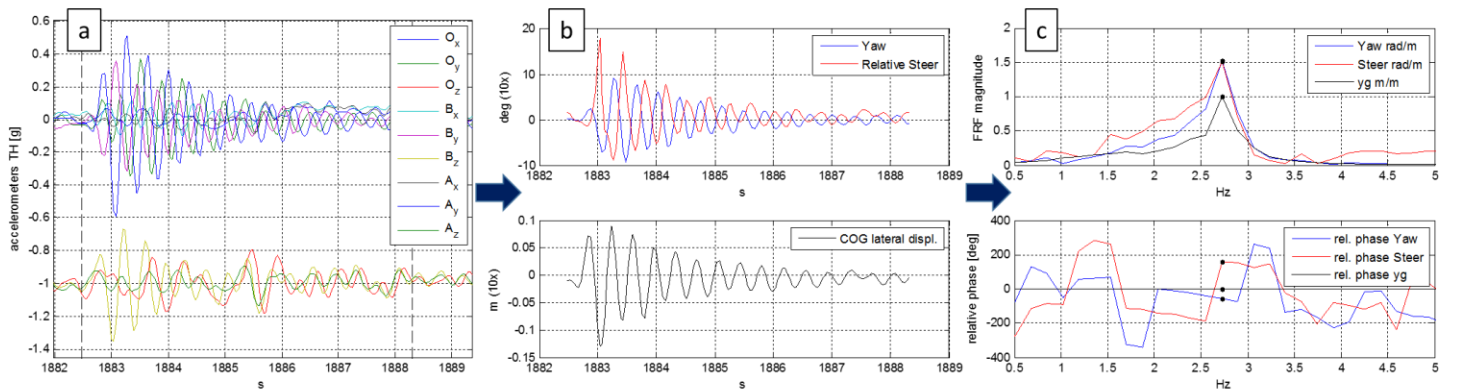


Figure 6 a) time histories of the three installed triaxial accelerometers during an impulse excitation: $A_{x,y,z}$ = steering head, $B_{x,y,z}$ = handlebar extremity and $O_{x,y,z}$ = tail. b) degrees of freedom calculation. c) FRF identification respectively in magnitude and phase with highlight on weave frequency (@ ≈ 2.7 Hz).

In figure 6, the sensors' signals time histories are reported (a), during an impulse excitation. Through geometry and trigonometrical manipulation, the DOFs time histories are identified (b). Finally, the frequency response functions, FRFs, are shown by means of magnitude (c-top) and phase (c-bottom). From time domain to frequency domain, each DOF magnitude has been nor-

malized over lateral displacement: this explains why lateral displacement has unitary module and relative phase equal to zero.

In the shown example, we detected the weave mode at frequency ≈ 2.7 [Hz] (a); thus, the relative magnitude of yaw with respect to lateral displacement is identified (≈ 1.5 [rad/m]) and the relative phase (≈ -60 [deg]).

2.3. “oversteering” and “understeering” weave

Once the weave was characterized by means of the three DOFs, the polar plot (or compass diagram) was computed (Figure 7 (c)). This visualization allows to better visualize the Frequency Response Functions (FRFs) of the system, both in magnitude (a) and in phase (b).

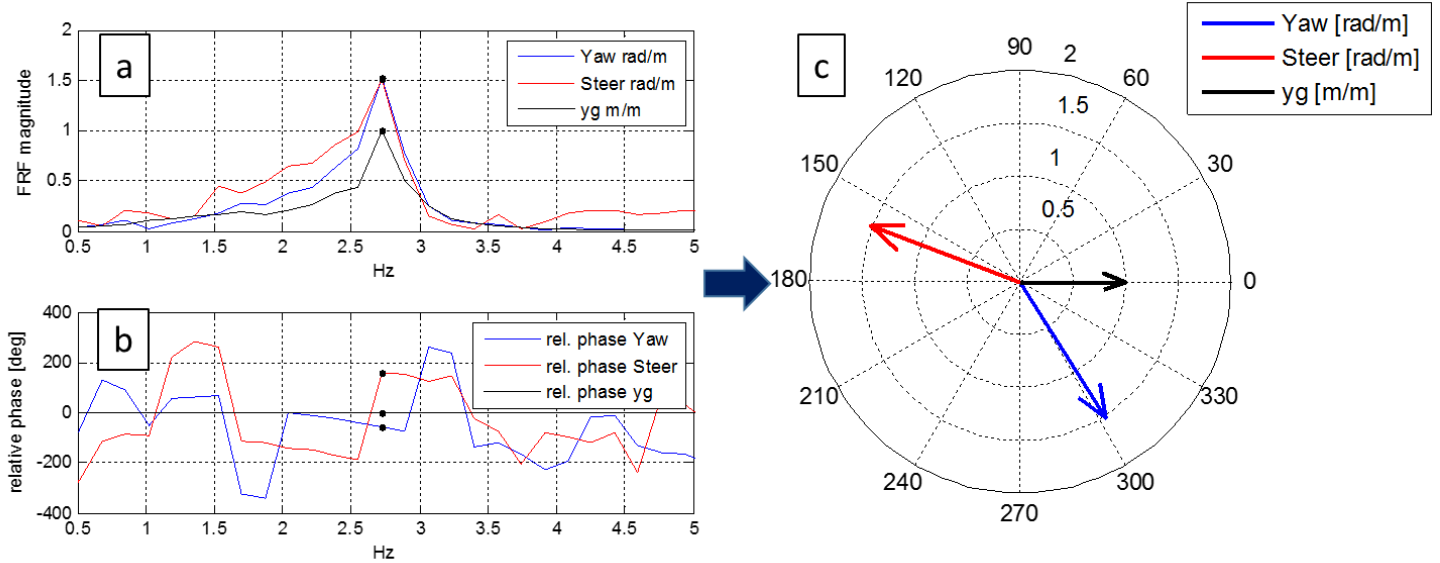


Figure 7 FRFs between degrees of freedom: (a) represents the magnitude normalized over lateral displacement while (b) the relative phase. (c) represents the polar plot or compass diagram.

In the compass diagram, each DOF is represented by an arrow; the length represents the module while the phase is given by the angle with respect to the horizontal. From time domain to frequency domain, as already anticipated, we compute each DOF magnitude normalization over lateral displacement: this is clearly visible in the compass diagram, too, where the black arrow, the lateral displacement, has unitary module and relative phase equal to zero.

The same information presented in the previous paragraph are visible in the compass plot (Figure 7 (c)).

For each time instant, the orthogonal speed components of the two main body’s extremities were plotted (Figure 8 (a), red arrows). From the two components, the resultant absolute velocity is computed (green arrows). Finally, the orthogonal line to the two resultants vectors is traced to determine the Instant Center of Rotation (ICR; red dot in Figure 8 (a)). By considering different time instants of the oscillation, it is possible to get the complete path followed by this entity during the oscillating period. The path described is the so-called Centrode [5] (red dots in Figure 8 (b)).

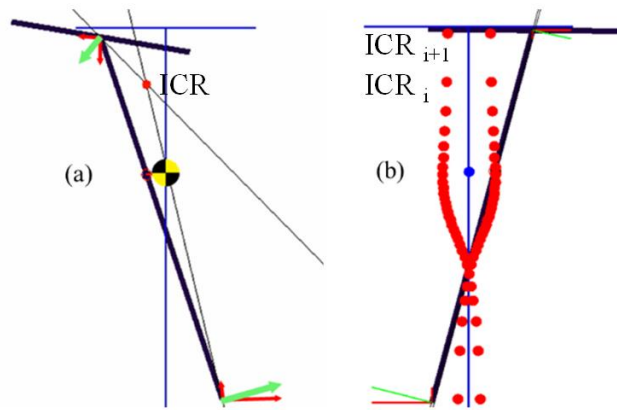


Figure 8 (a) ICR calculation. (b) Centrode calculation over weave oscillation period.

From Centrode analysis it is possible to identify different weave mode shapes. The relative phase among the DOFs could change consistently. This change leads to different bike behaviours that also the riders perceive. The Centrode analysis is the missing link in understanding critical situations where two motorcycles with same modal damping appears different at riders' opinion.

From experimental tests, it is possible to distinguish two weave mode shapes: the so-called “oversteering” and “understeering” weave. Figure 9 shows different weave modes built driving the relative phase between the lateral displacement and the yaw; magnitudes are maintained the same. The Centrode shapes is therefore represented. Whenever the yaw is in phase with lateral displacement, we named it “understeering” weave (the Centrode intersection falls behind the CoG). On the contrary, whenever the yaw is out-of-phase with lateral displacement, we named it “oversteering” weave (the Centrode intersection falls ahead the CoG).

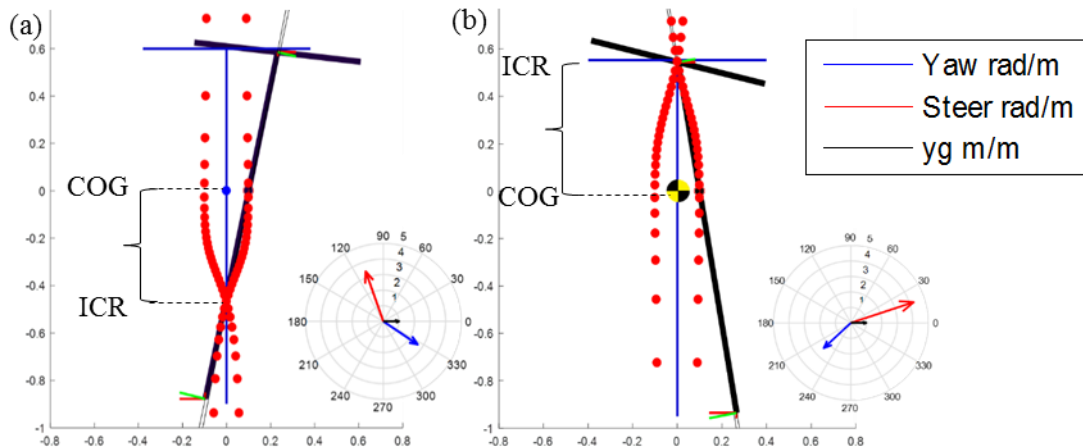


Figure 9 (a): example of “understeering” weave with yaw in-phase with lateral displacement: the centrode intersection point ICR meets below the CoG; (b): example of “oversteering” weave with yaw out-of-phase with respect to lateral displacement: the ICR meets ahead of the centre of gravity (CoG).

A numerical model has been used in order to generate artificial compass. The idea is to arbitrary set the magnitude and the phase of each DOF. Thus, it is possible to appreciate the contributes separately. In particular, while the yaw relative phase with respect to lateral displacement determines the intersection point of the centrode – and therefore the shape of weave (under/over steer weave) Figure 10, the yaw relative magnitude controls the distance between Centrode intersection and motorcycle's CoG (Figure 11): as the yaw relative magnitude increases (from (a) to (c)), the centrode intersection point get closer to motorcycle's CoG.

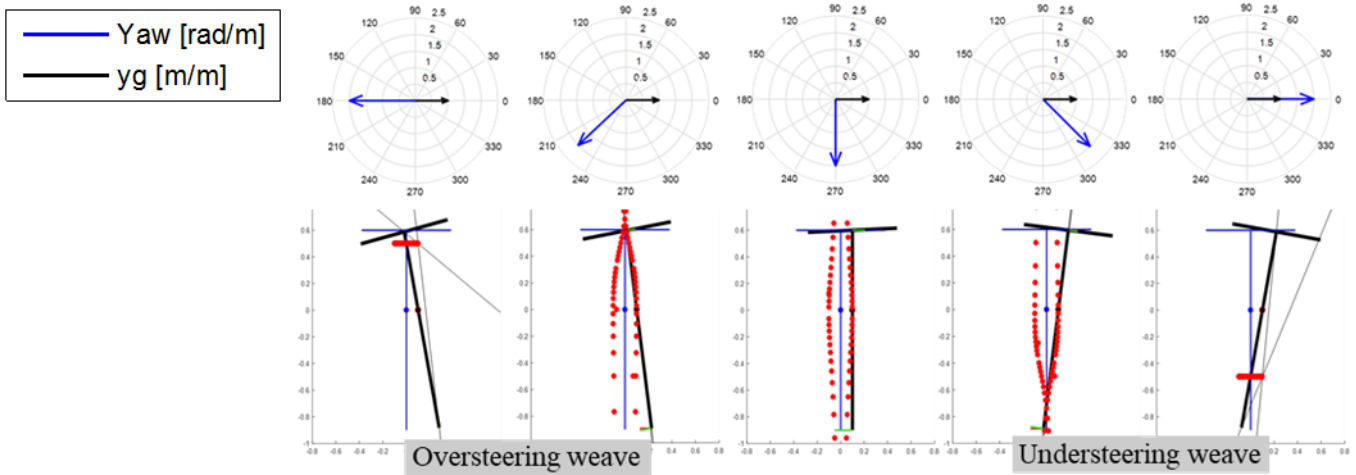


Figure 10: oversteering and understeering weave: yaw relative phase with respect to lateral COG displacement affects the shape of vibration.

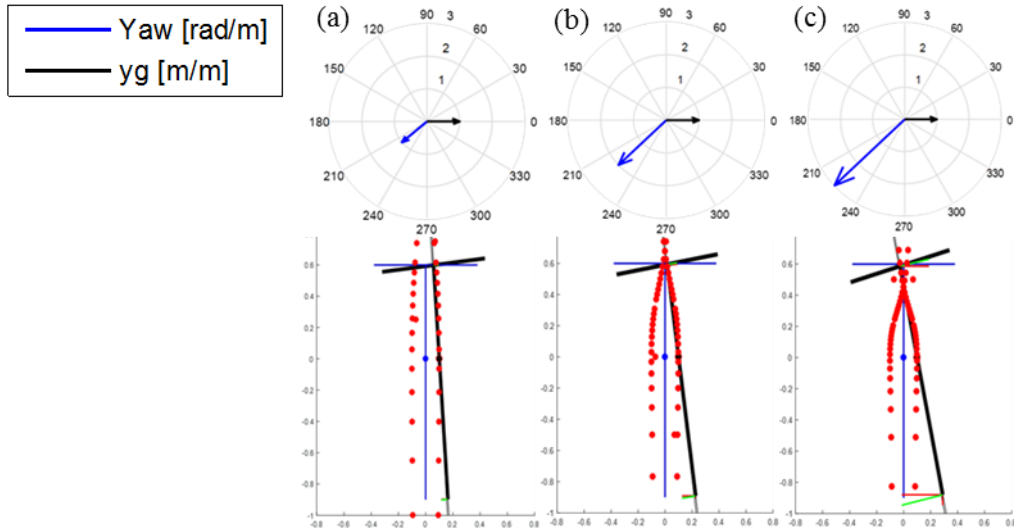


Figure 11: yaw relative magnitude effect on centre shape. This example shows an oversteering weave with yaw out-of-phase with respect to lateral displacement. As the yaw relative magnitude increases (same (a), twice (b) and triple (c) the magnitude), the centre intersection point gets closer to motorcycle's CoG.

These differences in modal shape create a different rider feeling. In fact, being oversteering weave characterized by relevant absolute steering angles, it requires a huge effort for riders to control the bike. In addition, being the rotation centre in front of the rider, his modal participation increases in counter direction with respect to steering head.

This generates an unpleasant feeling of probable falling. On the contrary, the steering behaviour shows mostly laterally translation and lower vibration magnitude during understeering weave. Being the absolute steering angles smaller, the rider needs to apply an easier control. The rider modal participation is reduced, reducing the perception of body oscillation and therefore increasing the perception of safety.

3. Experimental results

3.1. Modal damping and mode shape analysis

Three different crossover motorcycles were used for the experimental tests. The latter have different modal shapes that comes from different design choices. This topic will be further investi-

gated in next paragraph. The target is to quantify the effects of different payloads and speed conditions by using the mentioned methodology.

The vehicles were tested in three different payload conditions: only rider, rider with lateral side cases and rider with passenger plus lateral side cases. Figure 12 shows the trend of modal damping over the increasing speed range for different payload conditions for one of the vehicles under test (later on referred as Moto2).

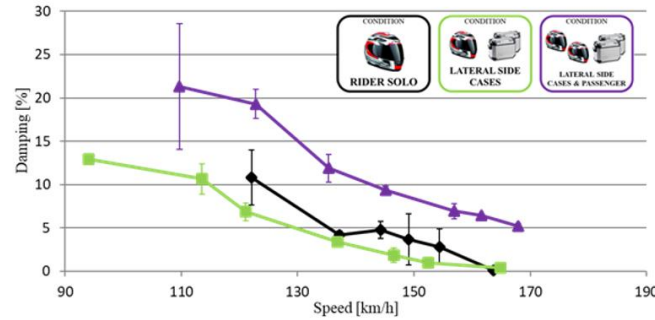


Figure 12: modal damping ratio for three different payload conditions over speed.

The green curve represents the lateral side cases configuration. With respect to the black curve, the rider-only set up, modal damping has decreased over each speed. This difference is higher at low and medium speeds. Purple curve represents modal damping adding the passenger. The passenger presence indices relevant improvements at each speed. Especially at high speeds, the passenger configuration is able to maintain the motorbike in a much safer range (e.g. in the specific case the modal damping ratio is about 5% @170km/h).

To sum up, lateral side cases worsen stability while passenger improves it.

Besides weave modal damping, weave modal shape is important as well. Figure 13 shows the modal shape analysis for the three different conditions at the maximum speed, the most critical for modal damping. (a) The modal shape analysis for the only rider (rider solo) condition: the centre shape is neutral, in fact the blue yaw arrow in compass diagram is delayed around 270 degrees from lateral displacement black arrow. (b) Rider plus side cases: the centre shape becomes understeering since intersection point lays behind CoG. The blue yaw arrow in compass diagram is delayed around 300 degrees (-60 deg) from lateral displacement. (c) Rider, passenger and side cases: the centre shape shows the most understeering behavior. Yaw magnitude increases and distance between CoG and Centrode intersection point reduces. Compass diagram shows a delay between lateral displacement and yaw around 330 degrees (-30 deg). In contrast with modal damping ratio results, both payload conditions improve motorcycle's stability, by means of modal shape. For the shown vehicle, increasing the payload, the motorcycle switches from oversteering to understeering behavior. In the compass diagram, the yaw relatively rotates counterclockwise.

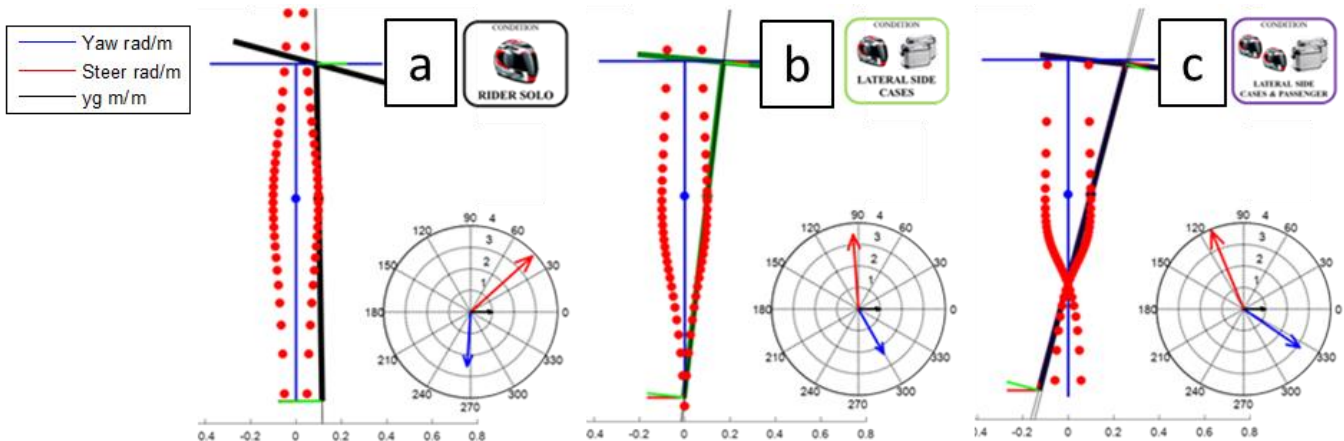


Figure 13: the modal shape analysis for three different payload conditions at the maximum speed. a) rider only, b) rider+side cases and c) rider+passenger+side cases.

To sum up, the payloads can have a double impact on motorcycle stability: lateral side cases decrease modal damping worsening stability but, at the same time, they improve the modal shape, giving safety feelings to the riders. Passenger instead, shows positive effects: both modal damping and modal shape are improved.

Figure 14 shows how the compass diagrams change over riding speed for one of the vehicles under test (Moto2).

Since the speed effect is independent from load condition, we reported a single case, chosen with lateral side cases as the most critical one. As it known from literature [2], increasing the speed means decreasing modal damping, so worsening stability.

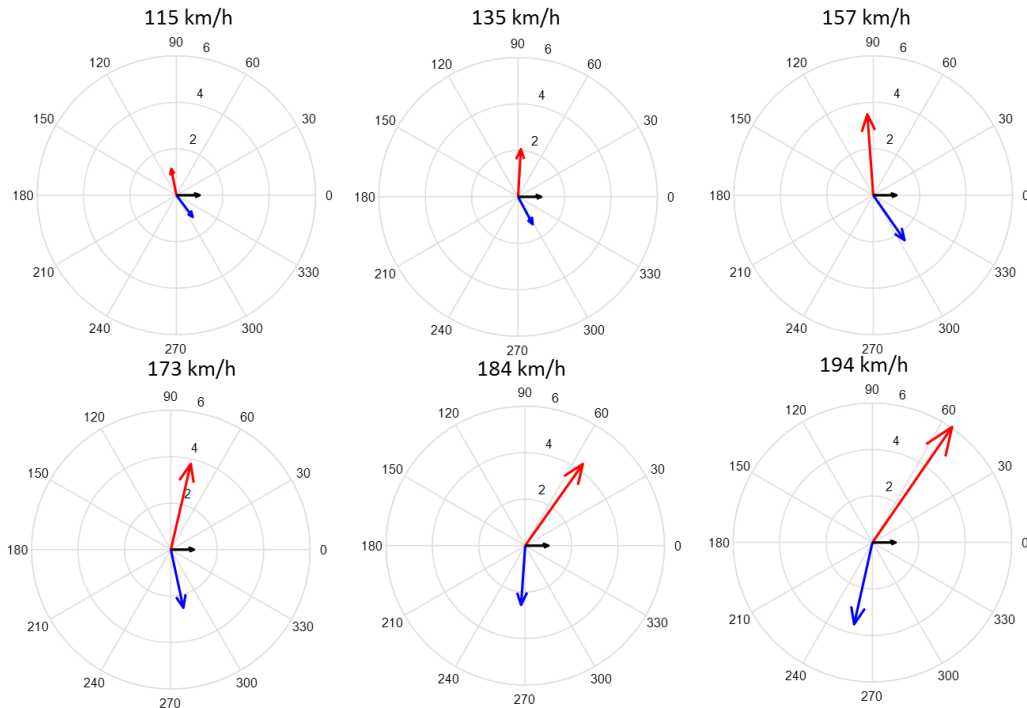


Figure 14: compass diagrams at different speed conditions: per rows: left to right; top to bottom = speed increasing.

Looking at the modal shape analysis through compass diagrams, increasing speed means increasing magnitude of relative steering and yaw. Moreover – and most important - the compass diagram rotates clockwise. This means from understeering to oversteering behavior, worsening stability.

Therefore, increasing speed leads only to negative effects on stability from both modal damping and modal shape perspective.

3.2. Results comparison between three different motorcycles

In previous paragraph we have seen the influence of payloads and speed on modal damping and mode shape. In particular, we explained how a weave understeering behaviour is always to prefer. Here we show further results comparing three different motorcycles focusing on mode shape. All of them belongs to crossover category and are from different manufacturers. All of them weights between 230 – 250 kg and reaches more than 450kg with passenger and luggage. From now on, those will be classified as Moto1, Moto2, Moto3. Those will be represented in orange, black and light blue respectively.

Is it true that all the bikes tested behave as the reference one presented in previous paragraph? Does the mode shape always tend to oversteering behaviour increasing speed? First of all, figure 15 shows the modal damping as function of the riding speed for the three crossovers, in the worst case: rider + side cases.

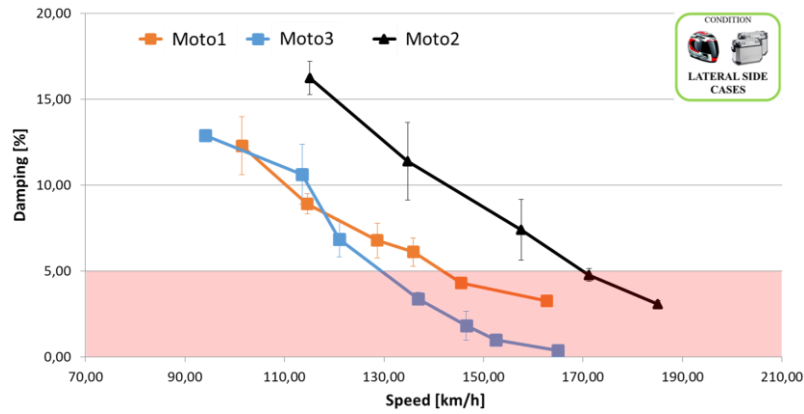


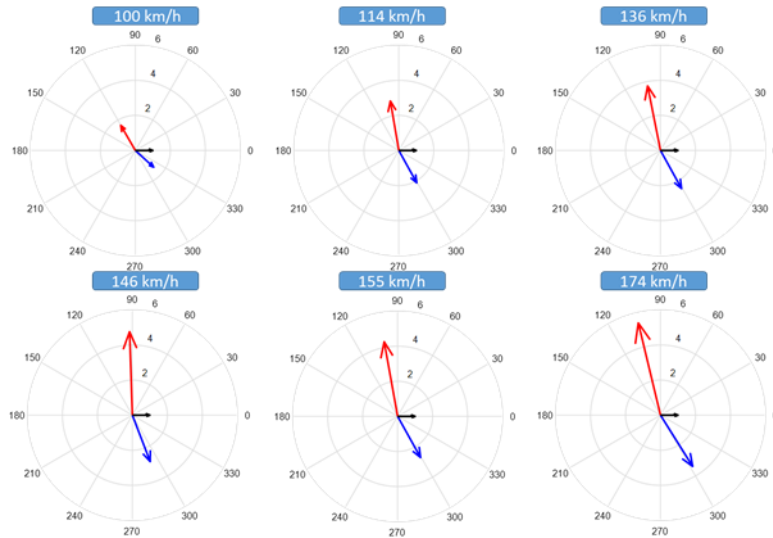
Figure 15: compass diagrams at different speed conditions for three different motorcycles, same load conditions (lateral side-cases).

Moto 2 appears to be better by means of stability, with a damping ratio higher over all the riding speed range.

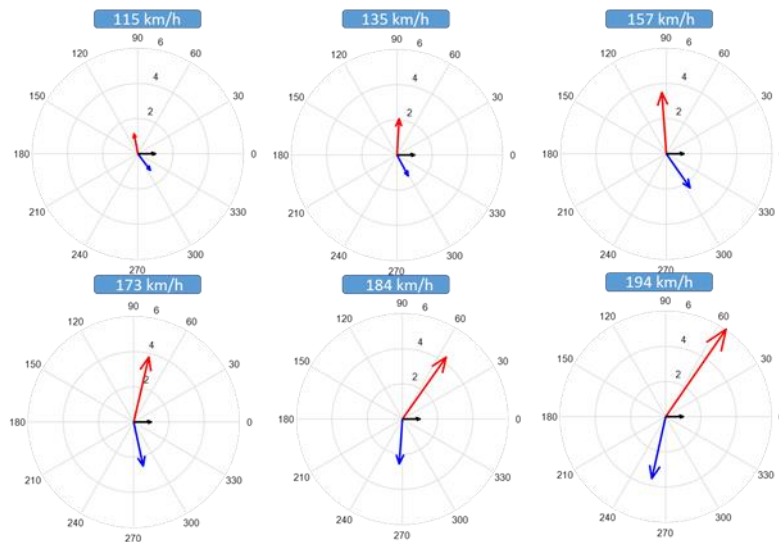
Figure 16 shows the compass diagrams comparison at four different increasing speeds for the three tested motorcycles. First of all, each vehicle shows an increasing of magnitude for yaw and relative steer with respect to lateral displacement (the higher the speed, the higher the arrows magnitude!). Regarding the mode shape evolution, instead, increasing speed, Moto1 and Moto2 show a detrimental oversteering effect since the blue yaw arrow rotates clockwise. Moto3, instead, shows no differences in terms of yaw phase.



Moto1



Moto2



Moto3

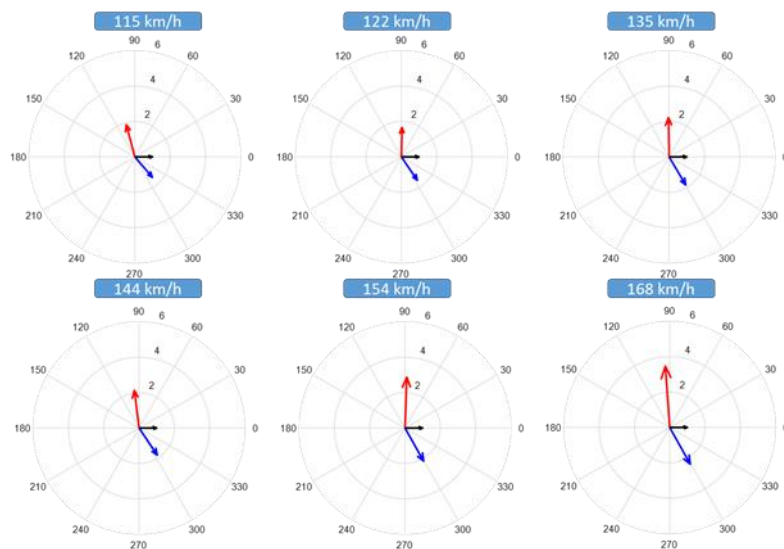


Figure 16: compass diagrams at different speed conditions for three different motorcycles, same load conditions (lateral side-cases).

These characteristics can be seen even looking at Figure 17 where the centroids are shown. Top to bottom, three centroids for each motorcycle increasing speed are shown. Moto1 and Moto2

show a shape evolution towards oversteering behaviour. The Centrode intersection point goes forward, to the top of the vehicle. Moto3 instead does not show any difference. The behaviour is always understeering and the vehicle does not show detrimental effects when the speed increases. This must be read as a positive effect.

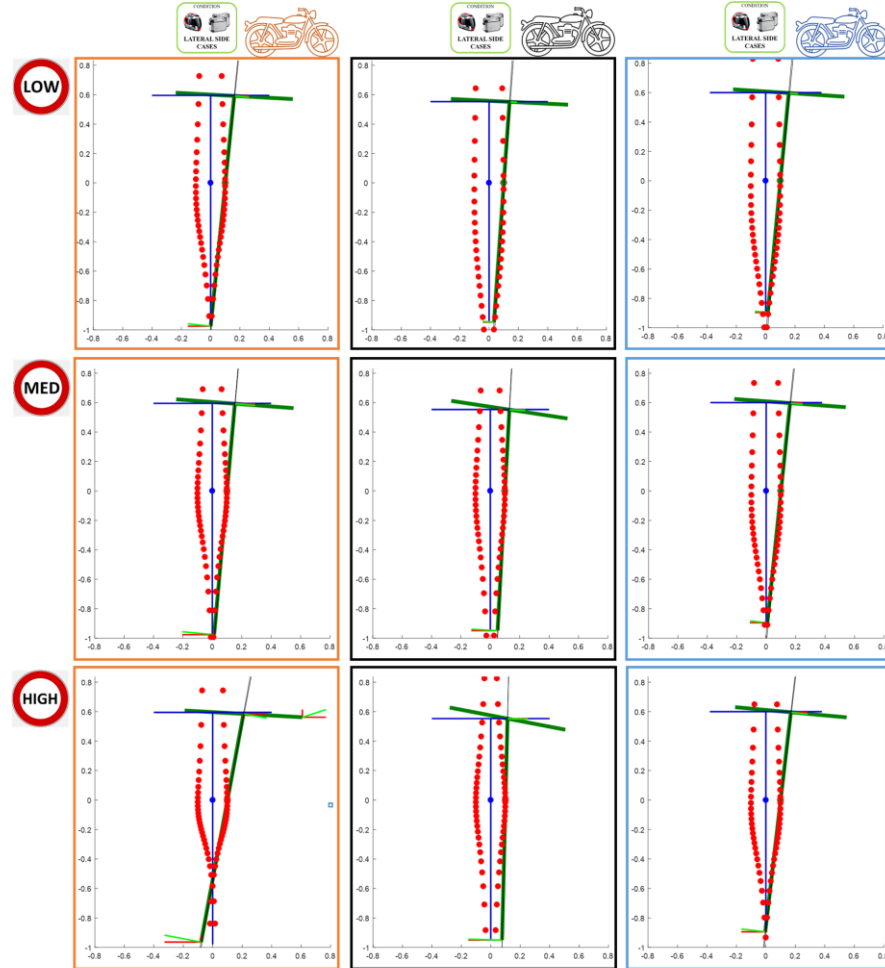


Figure 17: weave mode shape evolution over speed. Loaded condition (lateral side cases). Moto1, Moto2 and Moto3 represented respectively in orange, black and light blue. Top to bottom the speed increases.

After having seen the speed influences on mode shape, we want now to investigate the payload effects. Figure 18 shows the results for modal damping. The trend is confirmed. Passenger, always represented in purple, improves the unloaded condition, represented in black. Lateral side cases, instead, worsen the stability. Moto2 shows marginal differences between the two conditions of unloaded and loaded by side cases only.

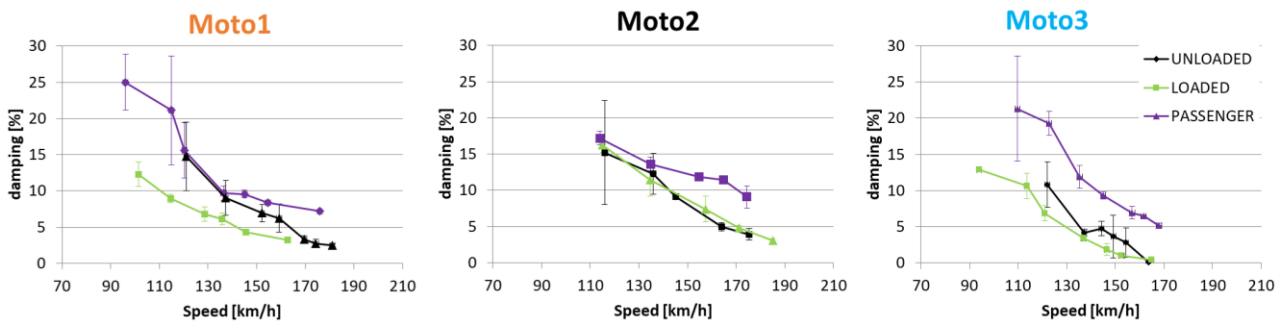


Figure 18: modal damping for three difference motorcycles. In black rider solo condition, in green loaded (lateral side cases), finally in purple the passenger and lateral side cases.

The most interest considerations regard the payload effects on modal shape. Figure 19 sums up the results. For the sake of clarity, we show a single speed for each condition. It has been chosen to show results at high speeds to emphasize the payload effects when the modal damping is low.

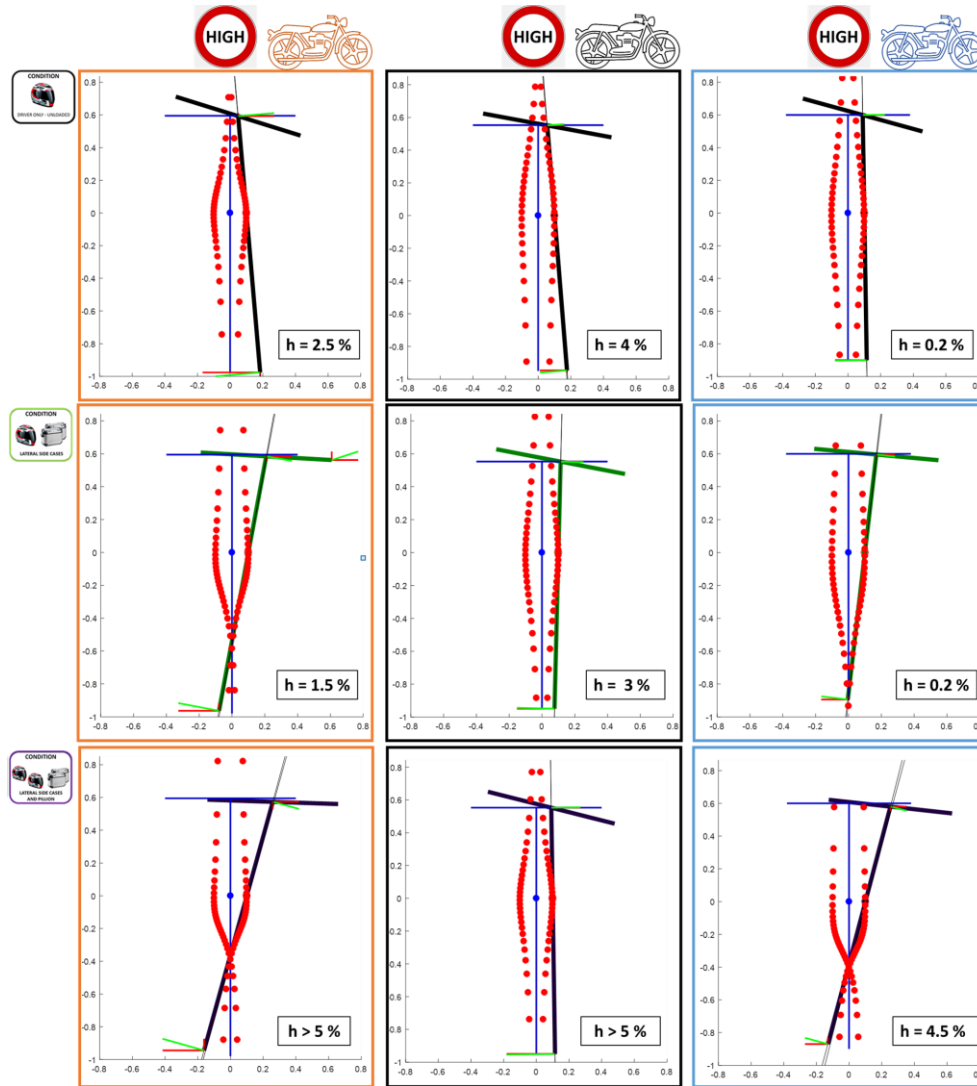


Figure 19: modal shapes for three difference motorcycles. Maximum speed available around 170 km/h. Top to bottom: rider solo condition, loaded with lateral side cases and loaded with lateral side cases and passenger. Left to right Moto1, Moto2 and Moto3.

As explained in previous paragraph, looking at the modal shape, the payload effect is different from what happens for modal damping. Starting from the first row of Figure 19, it can be seen how the three different motorcycles behave differently. Moto1 and Moto2 at the original unloaded condition, tend to be oversteering while Moto3 shows mostly a neutral behaviour. The modal damping ratio, $h[\%]$, is also displayed. The value enhances how Moto3 is already highly unstable with respect to the others; per row, in fact, Moto3 has always a lower value of modal damping at the same riding speed.

On the second row the loaded condition by lateral side cases is shown. The effect for all the vehicles is positive by means of modal shape, since the ICR meeting point goes backwards. Modal damping decreases instead.

Looking at the last row, the passenger configuration is represented. All the motorcycles show understeering behaviour with Moto1 and Moto3 highly enhanced. Also modal damping increases sensibly with respect to the side cases condition.

The riders gave an important feedback regarding the behaviour of the motorbikes. Moto3, even characterised by the worst performance for modal damping, was always preferred in terms of

perceived safety. Its modal shape was never recorded to be oversteering. This feedback confirms the importance to consider modal shape besides modal damping. Without considering the vibrational shape, Moto3 would be considered as dangerous while at the end it is not.

4. Numerical results

The second step of the work is aimed to numerically confirm the experimental evidences so to use a reliable model able to perform targeted sensitivity analysis to limit the in-field testing phase. A fully nonlinear, 20 DOFs multibody vehicle model has been implemented. In particular, these DOFs are:

- 6 DOFs for main frame (three absolute translation and rotations);
- 1 DOF for relative rotation around steering axis;
- 2 DOFs for rotational joint compliances (torsional rotation and lateral displacement of the front steering part with respect to main frame);
- 1 DOF for fork travel;
- 1 DOF for swing arm rotation around its pivot;
- 2 DOFs for swing arm compliances (flexural and torsional contributes);
- 1 DOF for rider relative roll angle (with respect to main frame);
- 1 DOF for passenger relative roll angle (with respect to main frame);
- 2 DOFs for side-cases lateral displacement;
- 1 DOF for top case lateral displacement;
- 2 DOFs for wheels spin (front and rear).

In order to reduce the computational effort, the structural stiffness and damping are modelled as lumped parameters. In addition, the most relevant choices were done around how to model rider and passenger. In terms of inertial properties, the lower parts of the bodies are embedded into the bike main frame. The upper parts instead are allowed to rotate around their own roll axes. They are passive systems, independent each other, characterized by dashpot elements. Modeling rider and passenger with a single DOF each was done accordingly to [6], [7], as well as for the proper choice of values of their lumped parameters.

4.1. Numerical results: experimental trend confirmation

The model previously described has been used to correlate the numerical and the experimental trend. In the following figures the numerical results are shown as black dots while, in red/orange (respectively for the rider solo and the rider+side cases condition), the experimental results are reported.

Numerical model confirms how the lateral side cases as an element that worse stability, decreasing the modal damping (Figure 20). The passenger instead, is confirmed to improve stability. However, at very high speeds the behaviour between experimental and numerical is less precise. The reason of that can be found in passenger modelling. He was modelled as a passive element characterized by lumped parameters. However, during our experimental tests, at high speeds, we noticed how difficult it is for the passenger to stay neutral when the weave vibration occurs!

Additionally, the parameters of the numerical model do not correspond exactly to the ones of the physical motorbike since those were not available at the time of the research. Plausible values have been assumed for the unknown quantities.

It is important to remark how, the numerical tool aims to replicate the trend over similar conditions. The simulation is then used to explore possible solutions to improve vehicle stability.

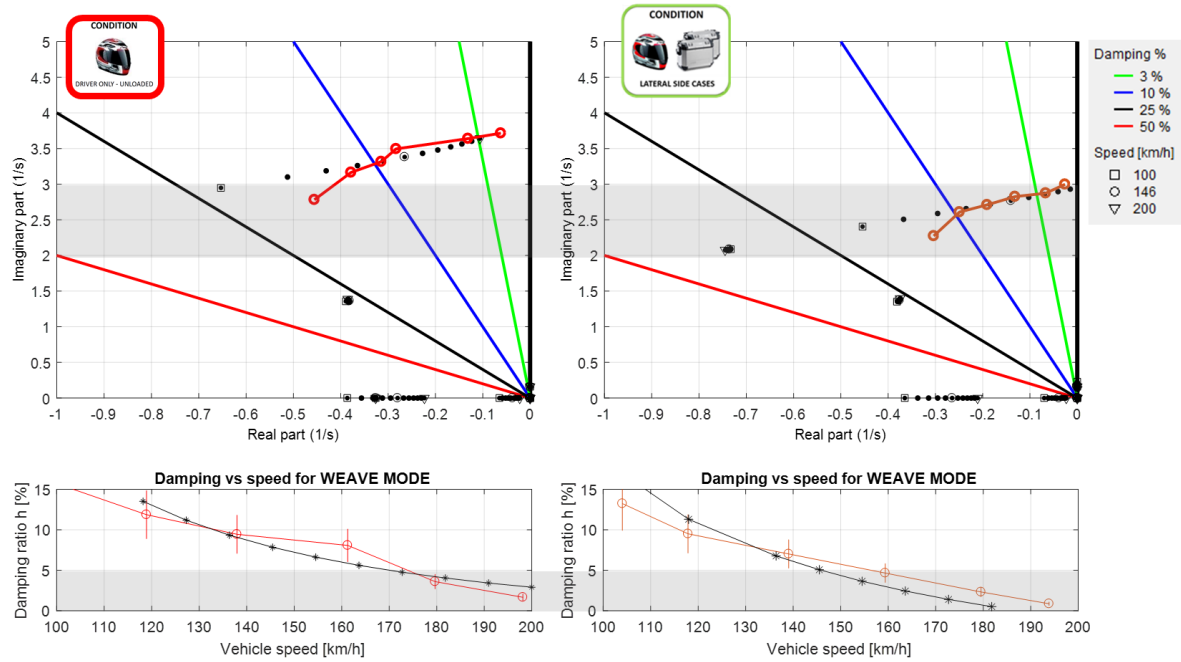


Figure 20: root loci and modal damping ratio vs speed; comparison between experimental and numerical results for the riding solo condition (left) and the most critical condition of rider+side cases.

Table 1 shows the comparison between experimental and numerical model, looking at modal shape through compass diagrams. Adding payloads, the yaw blue arrows rotate counter clockwise in both experimental and numerical results. This lead to an increase of stability feeling for riders, confirmed by the subjective judgments.

As anticipated, still some differences occur between numerical and experimental results. In particular, for what concerns the relative angle: the yaw is in-phase with the lateral displacement, but the magnitude is slightly different. Reported differences are due to the fact that the parameters of the numerical model do not correspond exactly to the ones of the physical motorbike since not all the vehicle data were available¹.




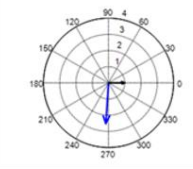
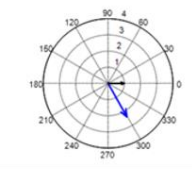
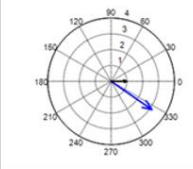
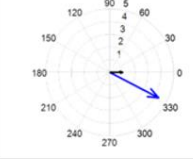
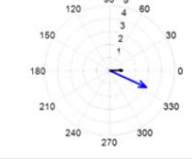
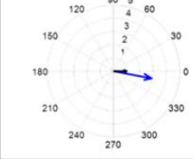
	 Rider Solo	 Lateral Side Cases	 Lateral Side Cases & Passenger
Experimental			
Numerical			

Table 1 effects of payloads on modal shape: experimental and numerical results.

The evidences of reliability of the numerical model with respect to the experimental trend allow using the numerical model to perform targeted sensitivity analysis to limit the in-field testing phase. The last paragraph will show an example of relevant results obtained through it.

¹ For those unknown parameters, the numerical model has been used to try to identify plausible values by following iterations.

4.2. Numerical results: targeted sensitivity analysis

Among all the possible results, we decided to present in detail few significant examples of sensitivity analysis done with the numerical model previous described. By changing the CoG position of pillion and the lateral side cases mass and position the effects on stability are different. As it can be observed in Figure 21, a proper design of the motorbikes' pillion longitudinal position (variable named Bpp and measured in [m]) leads to a better stability. In particular at medium speed, at about 150km/h (circular dots), the computed weave modal damping ratio of the nominal configuration is about 12%. When moving forward the passenger longitudinal position in the riding direction of 20% with respect to the nominal value (from 0,70 to 0,56 [m]), the damping ratio reduces to 10%, while it is improved to about 15% (+25% of improvement vs nominal) when moving the same quantity backward (from 0,70 to 0,84 [m]).

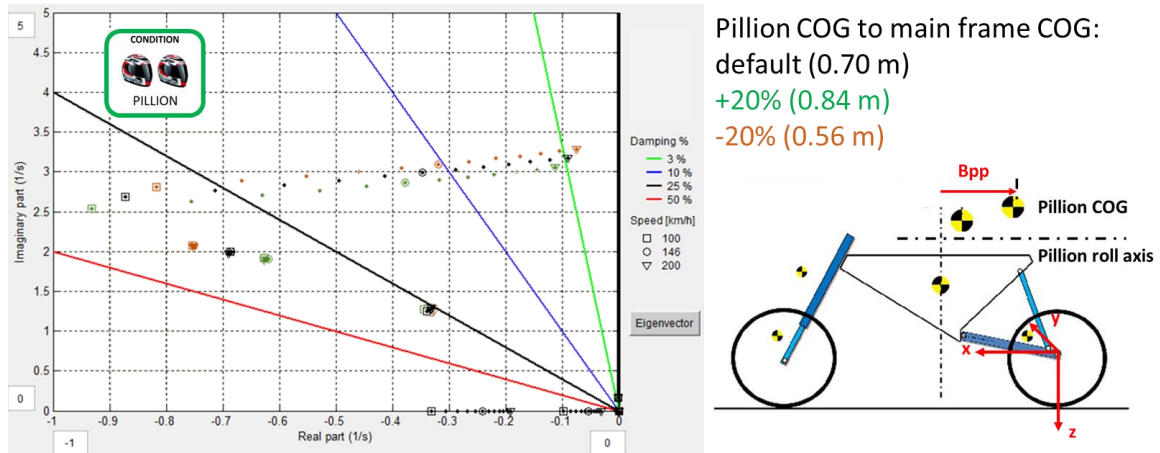


Figure 21: effect on weave modal damping of the pillion CoG longitudinal position with respect to riding.

Figure 22 shows the sensitivity analysis when moving the pillion up or down. The higher the pillion is, the more the weave is stabilized. Riding at about 150km/h, the damping ratio rises from 10% (when pillion height is 0,136m from the rolling axis) to 13% (when the same quantity is set to 0,17m).

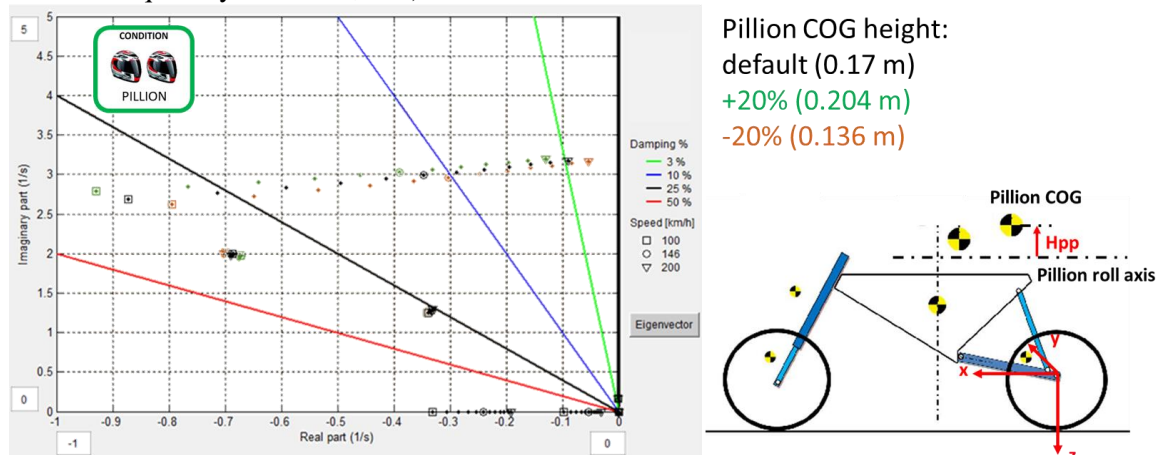


Figure 22: effect on weave modal damping of the pillion CoG height.

Concerning the luggage CoG, if the longitudinal position seems not to affect the motorbike' stability, the overall mass and the height do. In figure 23 it is possible to appreciate the effect of the side cases mass. The lower the mass, the more damped the weave is.

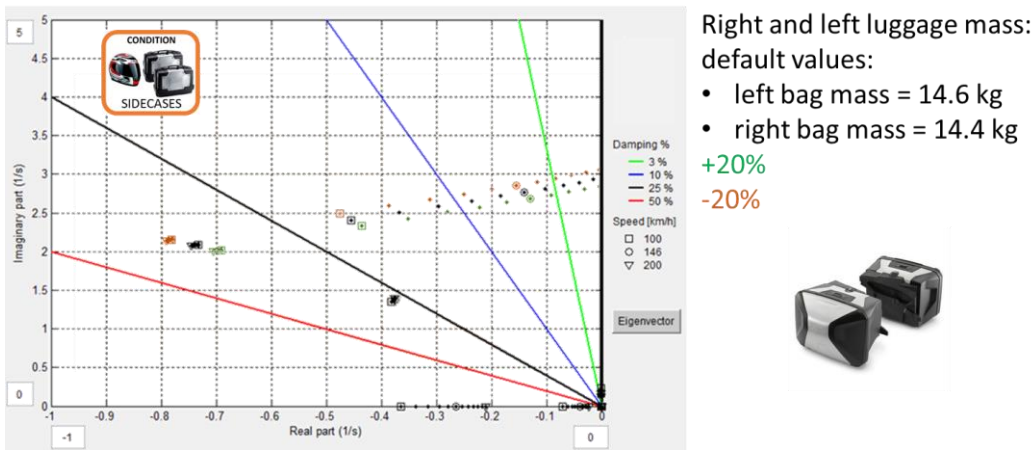


Figure 23: effect on weave modal damping due to the side cases' overall mass.

In figure 24, the vertical position of the side cases is investigated. Increasing the side cases height, a benefit in terms of stability occurs.

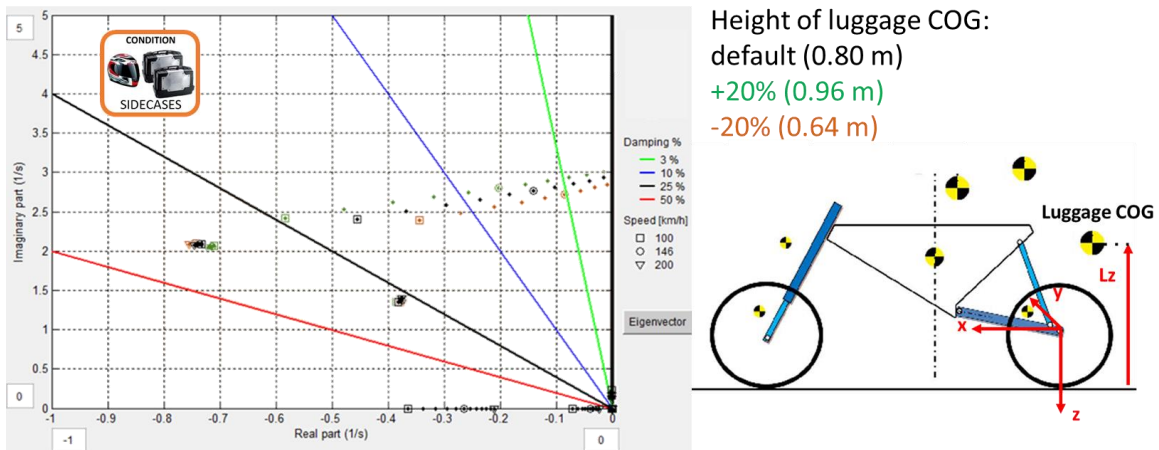


Figure 24: effect on weave modal damping due to the side cases vertical position from ground.

Besides the above examples, figure 25 sums up all the parameters to take care of during motor-cycle preliminary design. If, obviously, the weight of the passenger is not up to the designer, elements such as the position of the pillion and the position of the side/top cases are significant to improve riding stability. In yellow are represented the improvements regarding pillion; in blue the ones for lateral side cases. In particular, the yellow arrows suggests how the passenger CoG should be moved upward and backward and, the heavier the passenger is, the better it is for weave stability. Concerning the lateral side cases, CoG should be moved upward; moreover, the lighter the luggage the higher the weave stability.

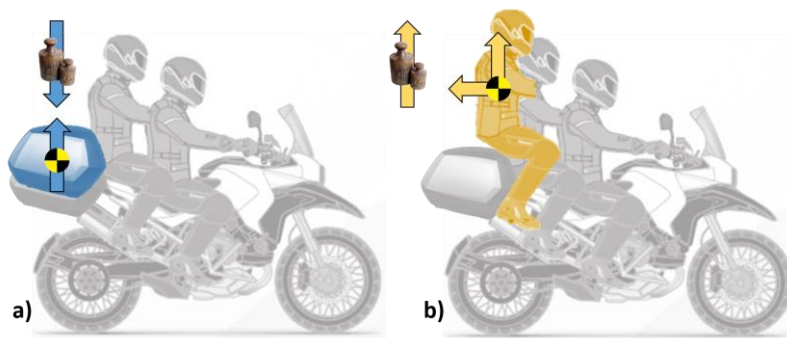


Figure 25: improvements directions for lateral side cases (a) and pillion design (b).

5. Conclusion

The target of the research was to improve the rider safety related to dynamic instability. In order to achieve the target, several experimental evidences have been acquired by on-field tests. By the installation of multiple accelerometers and dynamic sensors, the experimental identification of the weave vibration mode has been carried out for different vehicles, payload conditions and different riding speeds. The question piloting the research was: "... can two different vehicles, having the same weave modal damping, but characterized by a different vibration mode, being differently rated by users?...". The answer is affirmative.

It followed how it is needed to consider also the shape of vibration besides modal damping as stability indicator. Some relevant results were shown, highlighting the distinguishing between a better and a worse rider feeling called respectively "*understeering*" and "*oversteering*" weave. In particular, we have focused on the Centrode shape analysis by means of the so called "*T-bike*" model and compass diagrams.

The next step was investigating experimental results about payload effects on motorcycle stability. We focused on lateral side cases and passenger effects on both modal damping and modal shape perspective. It followed how lateral side cases decreases the modal damping but, on the other hands, improve the weave modal shape. Passenger, instead, has only positive effects, improving at the same time both modal damping and weave modal shape.

The second stage was aimed to numerically confirm the experimental evidences so to use a reliable model able to perform targeted sensitivity analysis to limit the in-field testing phase. A fully nonlinear, 20 degrees of freedom (DOFs) vehicle model has been implemented, including tires, suspensions, structures' compliances and payload, such as rider, passenger, lateral side-cases and top case. The numerical model confirmed the numerical trend highlighting the payload role in motorcycle stability.

The weave modal shape analysis here introduced for the first time, want to be a new relevant tool to help in designing safer motorcycles. The designer, by using numerical models as the one we have proposed, could reach several advantages. The most relevant is figuring out which geometrical parameters and inertial properties most affects the modal shape and the modal damping at different speeds. A relevant example related to pillion CoG position was shown.

As future developments, the investigation on the numerical vs experimental correlation of the weave shape is ongoing. Additional experimental sessions are planned with more and more riders in order to deeper investigate the rider feeling when exposed to weave phenomena.

References

- [1] United Nations Economic Commission for Europe, UNECE Transport Review of Road Safety, First Edition, November 2008.
- [2] V. Cossalter, Motorcycle Dynamics, LULU, 2007.
- [3] H. Sumali, R.A. Kellog "Calculating damping from ring-down using Hilbert transform and curve fitting" IOMAC 2011, Istanbul, Turkey.
- [4] L. Klaus "Comparison of Hilbert transform and sine fit approaches for the determination of damping parameters" XXI IMEKO World congress, Prague, Czech Republic.
- [5] H. D. Eckhardt "Kinematic Design of Machines and Mechanisms" McGraw-Hill (1998) p.63.
- [6] A. Doria, M. Formentini, M. Tognazzo "Experimental and numerical analysis of rider motion in weave conditions", Vehicle System Dynamics 2012.
- [7] M. Formentini "Studio sulle instabilità dei motocicli alle alte velocità" PhD thesis XXIII ciclo (in Italian).